Chapter 22

Similarity Solutions of Unsteady Viscous Optically Thin Fluid Flow with Variable Properties and Thermal Radiation

Adegbie, K. S. Afesomu, S. Bello, P. A. & Adewole A.
Corresponding author's email: ksadegbie@futa.edu.ng

ABSTRACT

The study examine the dynamics of unsteady viscous optically thin fluid flow, characterized by variable properties contingent upon temperature. Acknowledging the fluid's laminar and incompressible nature, the investigation employs the Cogley et al. approximation for integrating thermal radiation effects. Through the use of suitable similarity variables, the complex partial differential equations governing the physical model are converted into a more manageable system of ordinary differential equations. Given the infeasibility of exact solutions for this transformed set, the homotopy analysis method (HAM) is utilized for approximation purposes. The study meticulously analyzes how various control parameters, including the thermal conductivity variation parameter and the Brinkman number, influence the fluid's velocity and temperature profiles, presenting the findings through graphical representations. Notably, it is observed that both velocity and temperature distributions exhibit an increase in response to enhancements in the aforementioned parameters.

Nomenclature

y	Dimensional distance
η	Dimensionless distance
t	Dimensional time
τ	Shear stress
U_0	Moving velocity of the lower plate
μ	Dynamic viscosity

K	Thermal conductivity
k_0	Ambient thermal conductivity
T_0	Ambient temperature
T_w	Ambient temperature
C_p	Specific heat capacity
μ_0	Ambient viscosity
ρ	Fluid Density
u	Dimensional velocity
T	Dimensional temperature
q_r	Radiative heat loss
f	Dimensionless velocity
θ	Dimensionless temperature
R	Thermal radiation parameter
α	Dimensionless viscosity variation parameter
λ	Dimensionless thermal conductivity variation parameter
Br	Brinkman number
Pr	Prandtl number

INTRODUCTION

The preponderance of exact solutions identified within the domain of fluid mechanics is predominantly classified under similarity solutions, where there's a reduction in the count of independent variables by at least one. These solutions have been derived through a variety of methodologies, including the group-theoretic method, dimensional analysis, and the more heuristic ad hoc method involving free parameters. Among these, the group-theoretic approach stands as the most structured and methodical strategy for deriving similarity solutions, with dimensional analysis being regarded as a subset of this method. The intricate dynamics of unsteady viscous optically thin fluid flow, exhibiting variable properties, have captivated the interest of researchers extensively over recent decades. This keen interest is attributed to the broad spectrum of significant applications the study of such fluid flow finds across various scientific and engineering disciplines. These disciplines span geophysics, metallurgy, astrophysics, electronics, chemical engineering, aeronautics, and petroleum engineering, among others. Given the pivotal role this category of fluid flow plays in such a wide array of fields, numerous studies have been dedicated to exploring the behavior of unsteady

viscous optically thin fluids as they interact with objects of various shapes under different initial and boundary conditions.

Alam et al. (2019) embarked on an investigation concerning the unsteady flow within a converging channel, adopting a distinctive similarity approach that amalgamated temporal and spatial variables into a singular parameter pertinent to the flow problem. In the latter phase of their research, the aspect of convective heat transfer was scrutinized. Introducing variable wall temperatures into the equation unearthed two scenarios conducive to similarity solutions: the first scenario featured a linear wall temperature profile, while the second scenario presented an inverse linear wall temperature profile. The numerical outcomes of this study included variations in skin friction and Nusselt number along the wedge nozzle, alongside detailed mappings of velocity and temperature distributions within the boundary layer. Hossain et al. (2013) directed their investigation towards delineating the similarity solution for the laminar combined free and forced convective unsteady boundary layer flow adjacent to a porous vertical surface, incorporating both blowing and suction phenomena. Initially, the Boussinesq approximation was utilized to render the governing boundary layer non-dimensional partial differential equations more tractable. Following this, based on an exhaustive analysis, similarity transformations were employed to transmute these simplified coupled partial differential equations into a suite of ordinary differential equations. Mohammed (2016) dedicated his research to analyzing the flow of an incompressible fluid over an isothermal horizontal plate, employing similarity solutions to this end. This approach facilitated an understanding of the fluid dynamics and heat transfer characteristics associated with such flows, providing valuable insights into the behavior of fluids under varying thermal conditions and the influence of suction or blowing at porous boundaries.

Ali (2017) addressed the issue of similarity solution of MHD unsteady boundary layer flow along heat transfer past a moving wedge in a nanofluid using the Buongiorno model. Koriko and Animasaun (2017), examined a novel similarity solution for micropolar fluid flow problem on an upper horizontal surface of a paraboloid of revolution (UHSPR) considering the impacts of a quartic autocatalytic kind of chemical reaction. The theory of similarity solution was applied to determine the appropriate scaling for the proposed angular momentum

equation. These equations, together with the prescribed boundary conditions, were solved using a numerical technique known as the Runge-Kutta method in combination with the shooting method. Viscosity parameter, which depends on temperature, enhances the vertical velocity close to free stream but reduces the micro-rotation near the upper horizontal surface of the paraboloid of revolution. Additionally, the impact of the thermal radiation parameter on the temperature profile including heat transfer rate can be significantly influenced by the thickness parameter. Salawu et al. 2019 analyzed viscous dissipative unsteady Poiseuille flow of unsteady incompressible reactive fluid involving a two-step exothermic chemical reaction within a porous channel made of two parallel fixed walls of width with convective cooling. Similarity solutions for the evolution of polydisperse droplets in vortex flows was examined by Dagan et al. (2017).

Thermal radiation, the process of heat transfer through electromagnetic waves, plays a vital role in various engineering and scientific fields. It is prominently observed in daily phenomena such as the warming of the Earth by the sun. This form of heat transfer becomes increasingly significant in high-temperature engineering processes, influencing the design of equipment within fluid dynamics. Its importance extends across multiple engineering disciplines, including solar power, mechanical, aerospace, chemical, environmental, and space technology. Thermal radiation's impact on fluid flows is crucial in industrial applications such as nuclear power plants, gas turbines, glass production, and furnace design. It also plays a key role in cosmic flight aerodynamics, rocket propulsion systems, plasma physics, and the aerothermodynamics of spacecraft re-entry at high temperatures. Research in this area, including works of Adegbie et al. (2019); Kesavaiah and Devika (2020); Rani (2019) underscores the extensive implications of thermal radiation in enhancing our understanding and technological capabilities in these diverse fields.

Adegbie et al. (2019) carried out a study on the ohmic heating of viscous magnetohydrodynamic flow past a continuously moving plate, considering factors like buoyancy, thermal radiation, and viscous dissipation. The mathematical formulation represented a

modified physical model involving a set of three partial differential equations. To simplify the analysis, appropriate dimensionless variables were introduced, transforming the system into two coupled nonlinear ordinary differential equations. Thereafter, the derived dimensionless system of equations governing modified model were solved utilizing the Homotopy Analysis Method (HAM). The study revealed that the skin friction coefficient alongside heat transfer rate grow with higher thermal radiation values and shrink as viscous dissipation parameter value rises. Adegbie and Fagbade 2016 addressed magnetohydrodynamic forced convective flow in a fluid saturated porous medium with Brinkman-Forcehheimer model, which is an important physical phenomenon in engineering application. Bivariate spectral relaxation method (BSRM) proposed by Mosta seeks to decouple the original system of partial differential equation (PDEs) to form a sequence of equations that can be solved in a computationally efficient manner. The obtained solutions showed a significant effect of the flow control parameters on the fluid velocity and temperature respectively. Findings show that an increase in viscosity variation parameter, thermal conductivity parameters increase the flow velocity and temperature distribution in the boundary layer region. Increase in thermal radiation parameter leads to decrease in the local heat transfer rate but skin friction experienced increment.

Makinde and Animasaun, (2016) examined thermophoresis and Brownian motion effects on MHD bio-convection of nano-fluid with nonlinear thermal radiation and quartic chemical reaction on upper horizontal surface of a paraboloid of revolution, the combined effects of buoyancy force, Brownian motion, thermophoresis and quartic auto catalytic kind of chemical reaction on bio-convection of nanofluid containing gyrotactic microorganism over an upper horizontal surface of a paraboloid of revolution are analyzed. Seth et al. 2016 investigated unsteady MHD natural convection flow through a fluid-saturated porous medium of a viscous, in- compressible, electrically-conducting and optically thin radiating fluid past an impulsively moving semi-infinite vertical plate with convective surface boundary condition. Umavathi (2015) reported a detailed analytical and numerical investigation on free convection flow of viscous fluid

through a porous medium due to the combined effects of thermal and mass diffusion. Effect of temperature-dependent viscosity and thermal conductivity were investigated in the presence of first-order chemical reaction. The non-Darcy model is applied to define the porous matrix. The effects of viscous and Darcy dissipations are considered. The governing equations of continuity, momentum, energy, and concentration which are coupled nonlinear ordinary differential equations are solved analytically using regular perturbation method and numerically using Runge-Kutta with shooting method.

Bichi and Ajibade, (2020) accounted for the combined impacts of thermal radiation, viscous dissipation, and varying viscosity on natural convection unsteady Couette flow within a vertical porous channel. The study employed suitable similarity variables to transform the partial differential equations governing the fluid behavior into dimensionless ordinary differential equations (ODEs). The emerging equations were solved using the Adomian decomposition method (ADM). The study revealed that the fluid velocity including temperature exhibited an increase with higher Eckert number, thermal radiation, and viscosity parameter. Ajibade and Bichi, 2019 conducted a study on natural convective Couette flow amid a porous vertical channel, considering the simultaneous effects of thermal radiation and varying fluid properties. In the model, the fluid is taken to be optically dense, and all its physical properties are taken to be constant except thermal conductivity and viscosity which are varying with temperature. The non-linear Rosseland heat diffusion was employed, resulting in highly non- linear flow equations. The study found that the fluid velocity together with temperature increased with increment in thermal radiation parameter. Additionally, the temperature and velocity decreased with an increase in the thermal conduction.

Jha et al. (2016) conducted a thorough investigation on fully developed steady natural convection flow within a vertical annular micro-channel. The study focused on the impact of temperature-dependent viscosity and also considered the influence of temperature

jump and velocity slip at the surfaces of the annular micro-channel. The research revealed that increased viscosity parameter brings forth enhancement of both the velocity and skin friction within the annular micro-channel. Hafees and Ndikilar (2014) examined the flow of viscous fluid between two permeable parallel plates with fluid injection at the bottom and fluid suction at the top. The work dealt with a fluid flow which is steady, laminar, viscous, and incompressible. Pressure gradient present in the fluid generated uniform vertical flow i.e., the vertical velocity is constant everywhere in the field flow.

Kesavaiah and Devika, (2020) examined the issue of heat transfer and free convection Couette flow within two infinite porous plates incorporating the impact of radiation. Babu (2020) analyzed the magnetohydrodynamic unsteady viscous fluid flow between parallel plates possessing many tiny pores and angular velocity when the fluid is being sucked away through both walls at the same rate.

Ebiwareme et al. (2022) utilized the combination of Adomian decomposition method and Laplace transform to perform an analysis on unsteady incompressible fluid bordered by two parallel plates in motion with constant velocity. The nonlinear partial differential equation modeling the flow is first changed to a nonlinear ordinary differential equation using similarity transformation. The model parameters affecting the flow geometry are analyzed and exhibited in tables and graphs. Kudenatti et al. (2017) addressed the problem of similarity solutions of the magnetohydrodynamic boundary layer flow over a constant wedge within porous media. The governing nonlinear boundary layer equations have been transformed into a third order nonlinear Falkner-Skan equation through similarity transformations. This equation has been solved analytically for a wide range of parameters involved in the study. Various results for the dimensionless velocity profiles and skin frictions are discussed for the pressure gradient parameter, Hartmann number, permeability parameter, and suction/injection. A far-field asymptotic solution is also obtained which has revealed oscillatory velocity profiles when the flow has an adverse pressure gradient. The results show that, for the positive pressure gradient and mass transfer parameters, the thickness of the

boundary layer becomes thin and the flow is directed entirely towards the wedge surface whereas for negative values the solutions have very different characters. Also, it is found that MHD effects on the boundary layer are exactly the same as the porous medium in which both reduce the boundary layer thickness.

Soid et al. (2017) took on the challenge of studying the unsteady magnetohydrodynamic flow alongside transfer of heat on a contracting sheet with the inclusion of ohmic heating. The obtained solutions are influenced by several emerging parameters, among others are Eckert number, magnetic field parameter, the unsteadiness parameter, and Prandtl number. The results presented encompass velocity and temperature profiles, alongside local skin-friction coefficient and local Nusselt number. Notably, for the shrinking sheet scenario, two solutions are found to exist. Moreover, the study reveals that magnetic and also unsteadiness parameters have significant impact on the heat transfer fluid flow phenomena. These parameters contribute to raised skin friction coefficient and the rate of heat transfer.

Zaib et al. (2020) performed entropic analysis of mixed convective magnetohydrodynamic flows of radiative tangent hyperbolic blood biofluids conveying magnetite ferroparticles from a non-isothermal vertical fiat plate with the influence of thermal radiation. To make the governing equations less complex, relevant adjustments are considered to accurately transform the resulting partial differential equations into ordinary differential equations. The modified mathematical expressions are then solved using a numerical approach employing an efficient algorithm based on the bvp4c method. Unsteady magnetohydrodynamic mixed convective flow of water on a sphere with mass transfer was addressed by Jenifer et al. (2021). An implicit finite difference scheme, in conjunction with the quasi-linearization, was utilized to find non- similar solutions. Skin friction is hindered or at least delayed from vanishing by increment in mixed convection for both cases. That is, steady fluid flow and unsteady fluid flow. Skin friction and also heat transfer coefficients are raised with a rise in time or MHD parameter. Having been motivated and

inspired by all these published paper on similarity solutions and unsteady viscous flow, a deserted area in the body of knowledge is sighted. However, reporting the similarity solutions of unsteady viscous optically thin fluid flow with variable properties and thermal radiation has not been attempted; hence this study.

GOVERNING EQUATIONS

This study examines the unsteady parallel flow near a flat plate that suddenly begins moving at a constant velocity U_0 within its own plane. Characterized by viscous dissipation due to a high velocity gradient, the flow is considered fully developed and incompressible. Influences from pressure gradients and body forces on the flow are disregarded, and the no-slip condition at the boundary is assumed to apply. Both viscosity and thermal conductivity are presumed to vary with temperature. The plate temperature, denoted by T_w, is assumed to be higher than the ambient temperature T_0 of the fluid. Given these assumptions, the equations that model the physical scenario are as follows:

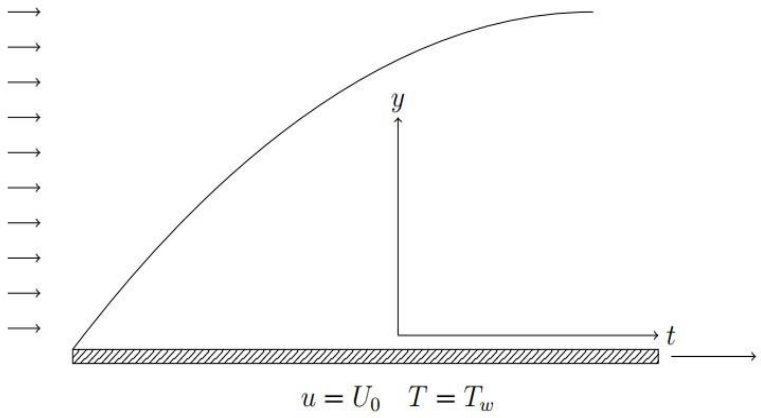

Figure 22.1: Schematic representation of the flow

Following the supposition above, the governing equations are formulated as follows:

$$\rho \frac{\partial u}{\partial t} = \frac{\partial}{\partial y}\left(\mu(T)\frac{\partial u}{\partial y}\right), \quad (1)$$

$$\rho c_p \frac{\partial T}{\partial t} = \frac{\partial}{\partial y}\left(K(T)\frac{\partial T}{\partial y}\right) + \mu(T)\left(\frac{\partial u}{\partial y}\right)^2 - \frac{\partial q_r}{\partial y}, \quad (2)$$

with initial conditions and boundary conditions:

$$u(y,0) = 0, T(y,0) = T_0 \text{ at } t = 0, \quad (3)$$

$$\begin{Bmatrix} u(0,t) = U_0, T(0,t) = T_w & \text{at } y = 0, \\ u(\infty,t) = 0, T(\infty,t) = T_0 & \text{at } y = \infty. \end{Bmatrix} \quad (4)$$

To carry out the similarity transformation of momentum equation, energy equation, initial and boundary conditions, the following similarity variables are adopted as:

$$\eta = \frac{y}{\sqrt{2vt}}, u(x,t) = U_0 f(\eta), \theta = \frac{T - T_0}{T_w - T_0}$$

The differential radiative flux term $\frac{dq_r}{dy}$ can be complex to model and for this reason, an algebraic approximation is utilized. The research of Cogley et al. brought forth a compact and numerically improvable mathematical expression. It was shown that in the optically thin limit, the fluid is not self-absorbing but will absorb radiation emitted by the confining boundaries (i.e., the continuously moving horizontal plates in this case) and it is taken that the fluid is optically thin possessing a relatively low density. The radiative heat flux is given by:

$$\frac{dq_r}{dy} = 4\gamma^2(T - T_0) \quad (5)$$

where γ denoted mean radiation absorption coefficient and is given by the following integral,

$$\gamma^2 = \int_0^\infty K_\gamma \left(\frac{\partial e_{b\lambda}}{\partial T}\right) d\lambda \quad (6)$$

Where K_λ is the absorption coefficient, λ is the wave length, and $e_{b\lambda}$ is the Planck function. In this present study, temperature dependent dynamic viscosity as in Adegbie et al. 2019 and Akinbobola and Okoya, 2015 can be expressed as:

$$\frac{1}{\mu(T)} = \frac{1}{\mu_0}[1 + \gamma(T - T_0)], \qquad (7)$$

which can still be written as:

$$\frac{1}{\mu(T)} = \sigma(T - T_r) \qquad (8)$$

where $\sigma = \frac{\gamma}{\mu_0}$ and $T_r = \left(T_0 - \frac{1}{\gamma}\right)$ are constants and their values depend on the reference state and the thermal properties of the fluid.

Also, following Salahuddin et al. 2020 and Opadiran and Okoya, 2021, temperature dependent thermal conductivity is adopted as:

$$K(T) = k_0\left[1 + \lambda\left(\frac{T - T_0}{T_w - T_0}\right)\right] \qquad (9)$$

Therefore, the dimensionless governing equations are:

$$\frac{d}{d\eta}\left[\left(\frac{\alpha}{\alpha - \theta}\right)\frac{df}{d\eta}\right] + \eta\frac{df}{d\eta} = 0, \qquad (10)$$

$$\frac{d}{d\eta}\left[(1 + \lambda\theta)\frac{d\theta}{d\eta}\right] + B_r\left(\frac{\alpha}{\alpha - \theta}\right)\left(\frac{df}{d\eta}\right)^2 - R\theta + P_r\eta\frac{d\theta}{d\eta} = 0, \qquad (11)$$

Subject to boundary conditions:

$$\left\{\begin{matrix} f = 1, \theta = 1, \text{at } \eta = 0, \\ f = 0, \theta = 0, \text{at } \eta \to \infty. \end{matrix}\right\} \qquad (12)$$

where

$\alpha = \frac{T_r - T_0}{T_w - T_0} = -\frac{1}{\gamma(T_w - T_0)}$ is the viscosity variation parameter

$Pr = \frac{\rho\nu C_p}{k_0}$ is Prandtl number

λ is the thermal conductivity variation parameter

$Br = \frac{\mu_0 U_0^2}{k_0(T_w - T_0)}$ is the Brinkman number

$R = \frac{4\gamma^2(2\nu t)}{k_0}$ is the thermal radiation parameter

METHOD OF SOLUTION: HOMOTOPY ANALYSIS METHOD

We will now solve (10), (11) with boundary conditions (12) by homotopy analysis method. In view of the boundary conditions (10), $f(\eta)$ and $\theta(\eta)$ can be expressed by the set of base functions of the form:

$$\{\eta^j \exp(-n\eta): j \geq 0, n \geq 0\}. \quad (13)$$

By the rule of solution expression, the solution of $f(\eta)$ and $\theta(\eta)$ can be represented in a series form as:

$$f(\eta) = \sum_{n=0}^{\infty} \sum_{j=1}^{\infty} a_{n,j}\, \eta^j \exp(-\eta j), \quad (14)$$

$$\theta(\eta) = \sum_{n=0}^{\infty} \sum_{j=1}^{\infty} b_{n,j}\, \eta^j \exp(-\eta j), \quad (15)$$

where $a_{n,j}$ and $b_{n,j}$ are constants.
We now construct the zeroth-order deformation equation as follows:

$$(1-q)L_f[f(\eta;q) - f_0(\eta)] = q h_f H_f(\eta) N_f[f(\eta;q), \theta(\eta;q)] \quad (16)$$

$$(1-q)L_\theta[\theta(\eta;q) - \theta_0(\eta)] = q h_\theta H_\theta(\eta) N_\theta[f(\eta;q), \theta(\eta;q)] \quad (17)$$

Next, we construct mth order deformation equation by differentiating (16) and (17) m times with respect to q and dividing it by $m!$

$$L_f[f_m(\eta) - \chi_m f_{m-1}(\eta)] = h_f H_f(\eta) D_{m-1}\left[N_f[f(\eta;q), \theta(\eta;q)]\right], \quad (18)$$

$$L_\theta[\theta_m(\eta) - \chi_m \theta_{m-1}(\eta)] = h_\theta H_\theta(\eta) D_{m-1}\left[N_\theta[f(\eta;q), \theta(\eta;q)]\right], \quad (19)$$

subject to

$$\left\{ \begin{matrix} f_m(\eta) = 1, \theta_m(\eta) = 1 \text{ at } \eta = 0, \\ f_m(\eta) = 0, \theta_m(\eta) = 0 \text{ at } \eta \to \infty, \end{matrix} \right\} \quad (20)$$

Where

$$\chi_m = \left\{ \begin{matrix} 0\ m \leq 1, \\ 1\ m > 1. \end{matrix} \right\} \quad (21)$$

Linear operators L_f and L_θ are defined as:

$$L_f[f(\eta;q)] = \frac{\partial^2 f(\eta;q)}{\partial \eta} - f(\eta;q), \tag{22}$$

$$L_\theta[\theta(\eta;q)] = \frac{\partial^2 f(\eta;q)}{\partial \eta} - \theta(\eta;q), \tag{23}$$

Initial guesses $f_0(\eta)$ and $\theta_0(\eta)$ are chosen as:

$$f_0(\eta) = \exp(-\eta), \tag{24}$$

$$\theta_0(\eta) = \exp(-\eta), \tag{25}$$

$$N_f[f(\eta;q),\theta(\eta;q)]\frac{d}{d\eta}\left[\left(\frac{\alpha}{\alpha-\theta(\eta;q)}\right)\frac{df(\eta;q)}{d\eta}\right] + \eta\frac{df(\eta;q)}{d\eta}, \tag{26}$$

$$\begin{aligned} N_\theta[f(\eta;q),\theta(\eta;q)] &= \frac{d}{d\eta}\left[\left(1+\lambda\theta(\eta;q)\right)\frac{d\theta(\eta;q)}{d\eta}\right] \\ &+Br\left(\frac{\alpha}{\alpha-\theta(\eta;q)}\right)\left(\frac{df}{d\eta}\right)^2 \\ &+Pr\eta\frac{d\theta(\eta;q)}{d\eta} - R\theta(\eta;q), \end{aligned} \tag{27}$$

$$D_{m-1}\left[N_f[f(\eta;q),\theta(\eta;q)]\right] = \frac{d^2 f_{m-1}}{d\eta^2} + \sum_{n=0}^{m-1}\left(\frac{1}{\alpha-\theta_{m-1-n}}\right)\sum_{k=0}^{n}\frac{df_{n-k}}{d\eta}\frac{d\theta_k}{d\eta} + \eta\sum_{k=0}^{m-1}\left(\frac{\alpha-\theta_{m-1-k}}{\alpha}\right)\frac{df_k}{d\eta} \tag{28}$$

$$\begin{aligned} D_{m-1}\left[N_\theta[f(\eta;q),\theta(\eta;q)]\right] &= \frac{d^2\theta_{m-1}}{d\eta^2} + \lambda\sum_{k=0}^{m-1}\theta_{m-1-k}\frac{d^2\theta_k}{d\eta^2} \\ &+\lambda\sum_{k=0}^{m-1}\frac{d\theta_{m-1-k}}{d\eta}\frac{d\theta_k}{d\eta} \\ &+Br\sum_{k=0}^{m-1}\left(\frac{\alpha}{\alpha-\theta_{m-1-k}}\right)\sum_{n=0}^{k}\frac{df_{k-n}}{d\eta}\frac{df_n}{d\eta} \\ &+Pr\eta\frac{d\theta_{m-1}}{d\eta} - R\theta_{m-1}. \end{aligned} \tag{29}$$

RESULTS AND DISCUSSION

Convergence Analysis of Solutions

By using Mathematica package BVPH 2.0, 10th order homotopy approximation of $f(\eta)$ along- side $\theta(\eta)$ are gotten when $\alpha = 0.1$, $\lambda = 0.5$, $R = 0.1$, $Ec = 0.1$, $Pr = 0.71$. In order to obtain the permissible values of auxiliary parameters h_f and h_θ, h-curves are drawn at 10th order homotopy approximations as shown in Figure 22.2 below:

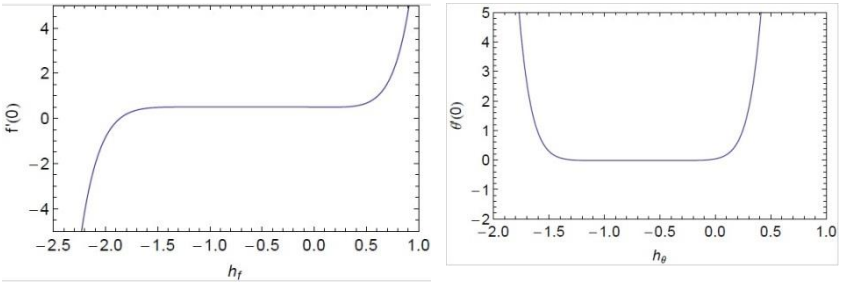

Figure 22.2: h_f −curve and h_θ −curve of $f'(0)$ and $\theta'(0)$ obtained at 10th order approximation respectively.

These figures show that the range for admissible values of h_f and h_θ are respectively $-1.50 \leq h_f \leq 0.25$ and $-1.15 \leq h_\theta \leq -0.20$. The optimal auxiliary parameters are approximately found to be $h_f = -0.3167$, $h_\theta = -0.4581$.

Discussion of Results

This part presents the repercussions of various emerging control parameters on the dimensionless velocity alongside dimensionless temperature in graphical forms (see Figure 22. 3 to Figure 22.12). Figure 22.3 and Figure 22.4 respectively exhibit the dimensionless velocity distribution and dimensionless temperature distribution under the influence of growing viscosity parameter when $\lambda = 0.1$, $Pr = 0.71$, $Br = 1$, $R = 0.1$. It is observed that an increase in α causes a decrease in velocity profile. Viscosity variation parameter is inversely proportional to temperature difference ($T_w - T_0$). Therefore, decrease in temperature difference results to a higher value of α. Physically, liquids with low temperature possess high viscosity which slow down the transport

of the fluid. Figure 22.4 shows that temperature profile exhibits the same pattern. It is observed that the temperature of the fluid decreases with increasing value of α. Physically, liquids with high viscosity move slowly and possess low temperature, hence the decrease in velocity and temperature of the fluid.

Figure 22.5 and Figure 22.6 show the effect of thermal conductivity variation parameter on both velocity profile and temperature profile respectively when $\alpha = 2$, $R = 0.1$, $Br = 0.1$, $Pr = 0.71$. It is evident that increase in the thermal conductivity parameter λ leads to increase in the velocity profile. Also, it is clear that an increase in the values of λ results in increase in temperature profile. This is expected because thermal conductivity is a direct linear function of temperature. Physically, increase in thermal conductivity parameter improves the heat conductivity of the fluid. Therefore, dimensionless temperature escalates since the heat conduction has improved and hence the increase in velocity. The effect of thermal radiation parameter R on dimensionless velocity profile and dimensionless temperature profile is shown in Figure 22.7 and Figure 22.8 respectively when $\alpha = 1.5$, $\lambda = 0.1$, $Br = 1$, $Pr = 0.71$.

Figure 22.7 shows that the velocity profile decreases as the radiation parameter ascends. Temperature profile is seen to descends with increase in thermal radiation parameter as shown in Figure 22.8. This is expected because increase in the value R induces greater emission of heat from the fluid by means of radiation. Dimensionless velocity and temperature distributions for varying Prandtl number is shown in Figure 22.9 and Figure 22.10 respectively when $\alpha = 2$, $\lambda = 0.1$, $R = 0.1$, $Br = 1$. Figure 22.9 shows that rising Pr leads to shrinking velocity. Physically, at a fixed value of specific heat capacity and thermal conductivity, increase in the value of Prandtl number Pr simply implies, increase in the magnitude of fluid viscosity. Equivalently, enhancing values of Pr means increase in viscosity but decrease in thermal conductivity. When the value of fluid viscosity is high this corresponds to fluid with low velocity.

Figure 22.10 shows the effect of Pr on temperature profile. It is obvious that the temperature profile is reduces as *Pr* increases. The reason is that higher values of Pr are equivalent to decreasing the thermal conductivity, and therefore decreases the thermal diffusivity which leads to the decrease of the energy transfer ability. The effect of increasing value of Br on velocity profile and temperature profile is visible in Figure 22.11 and Figure 22.12 respectively when $\alpha = 1.6$, $R = 0.1$, $\lambda = 0.1$, $Pr = 0.71$. It evident that the velocity profile ascends as the value of *Br* increase. Also, temperature distribution increases as a response to increment in Brinkman number *Br*. Physically, boost in the temperature of the fluid is credited to the internally generated heat added by the working fluid due to viscous dissipation. Consequently, the fluid experiences swift transport due to decrease in velocity as a result of growing temperature.

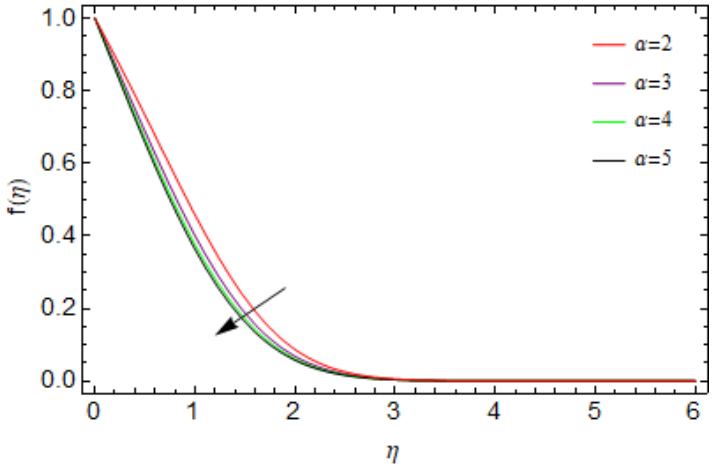

Figure 22.3: Effect of viscosity variation parameter on velocity

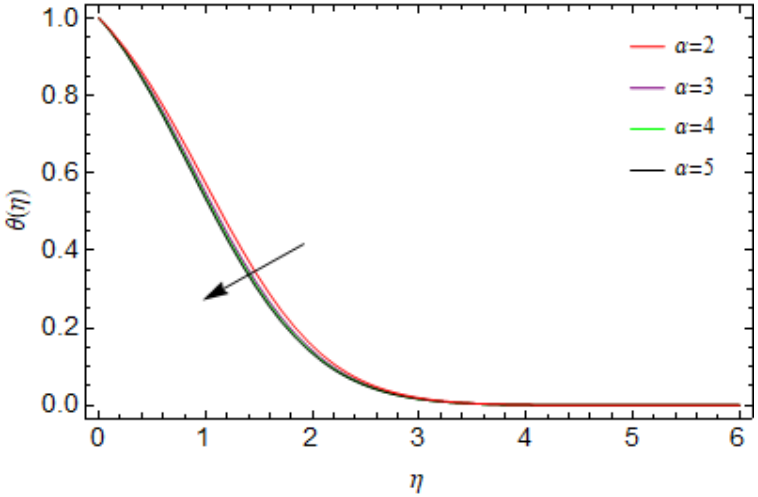

Figure 22.4: Effect of viscosity variation parameter on temperature

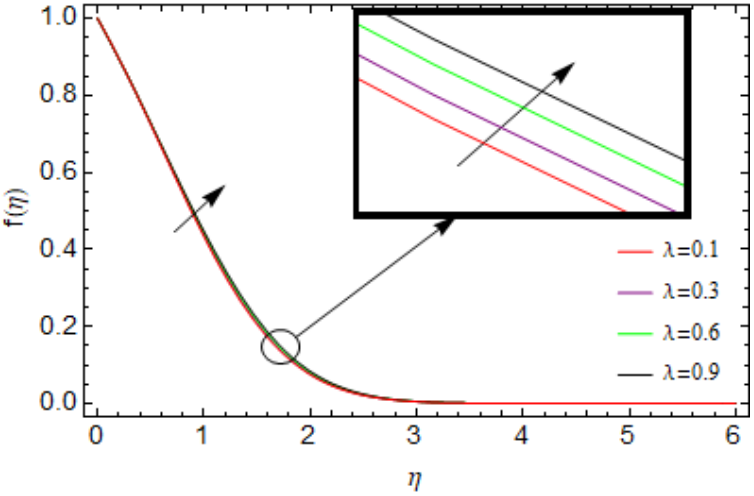

Figure 22.5: Implication of thermal conductivity parameter on velocity

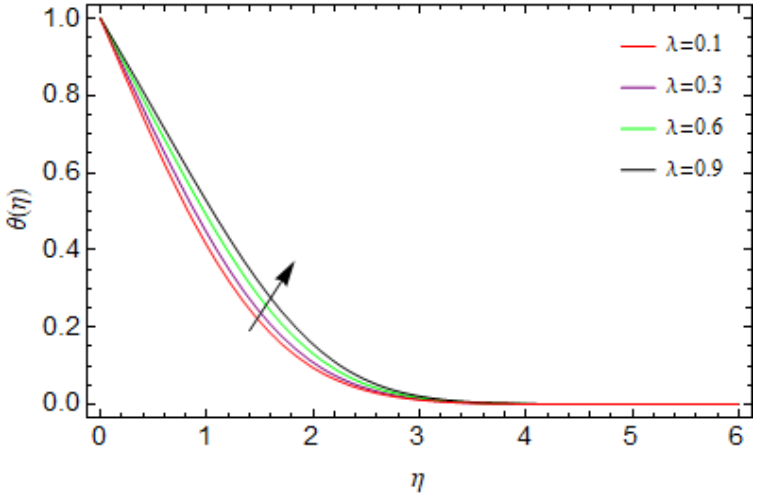

Figure 22.6: Implication of thermal conductivity parameter on temperature

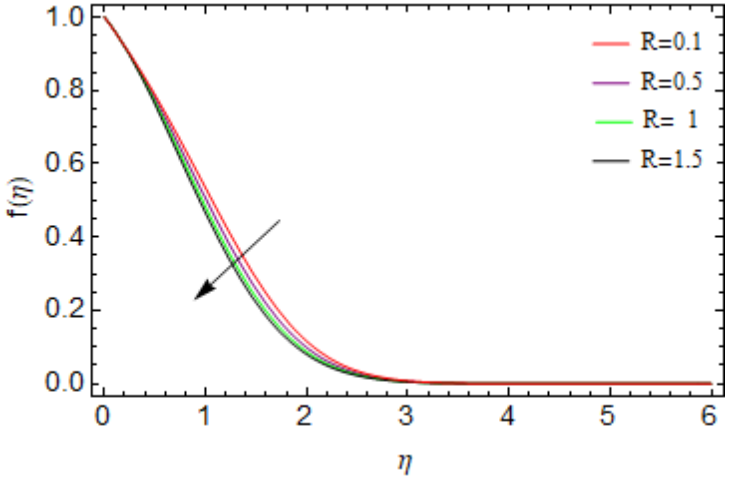

Figure 22.7: Effect of thermal radiation parameter on velocity

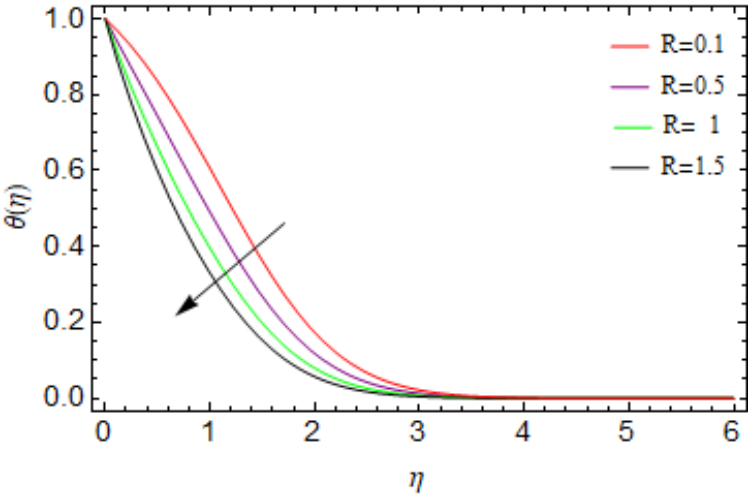

Figure 22.8: Effect of thermal radiation parameter on temperature

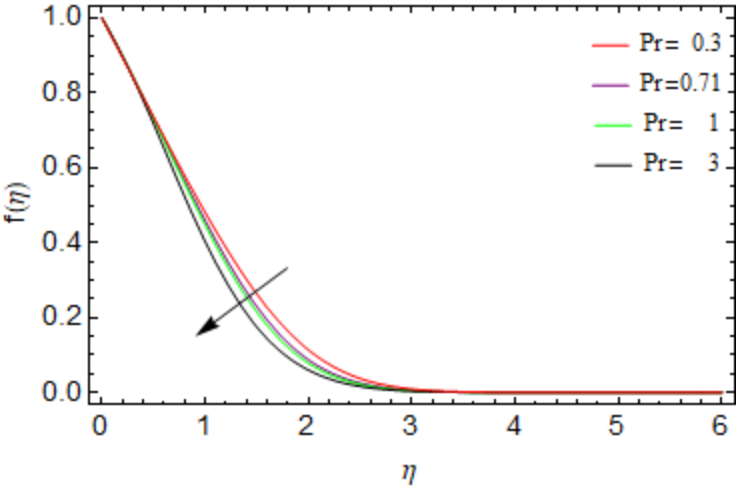

Figure 22.9: Influence of various Prandtl number on velocity.

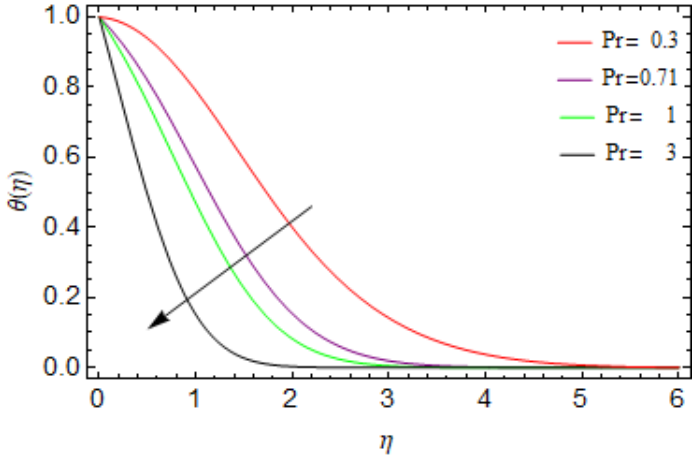

Figure 22.10: Influence of various Prandtl number on temperature.

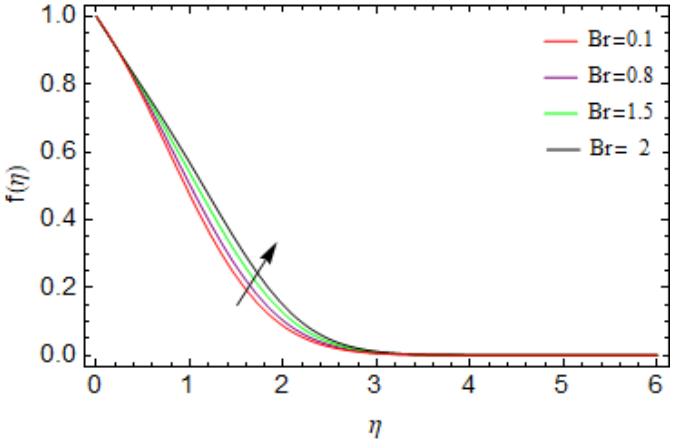

Figure 22.11: Velocity profile for varying Brinkman number.

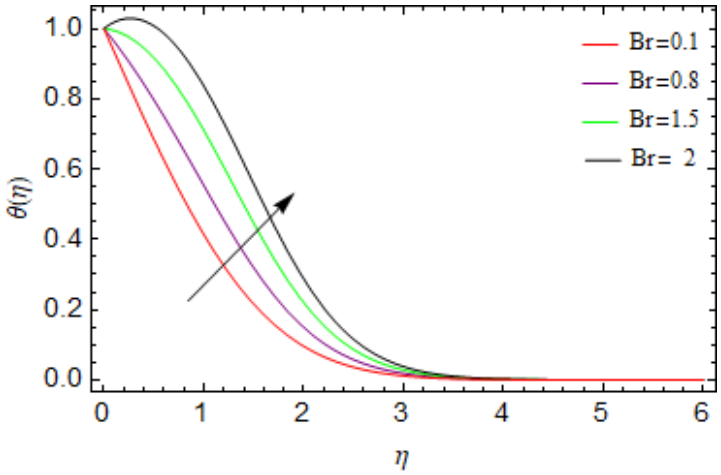

Figure 22.12: Temperature profile for varying Brinkman number.

CONCLUSION

Similarity solutions for unsteady viscous optically thin flow, considering the effects of temperature-dependent viscosity and thermal conductivity along with heat loss through thermal radiation, have been thoroughly investigated. The viscosity was modeled as inversely proportional to temperature, while the thermal conductivity of the fluid was considered a linear function of temperature. The study applied the Cogley et al. approximation for modeling radiative heat loss and employed the homotopy analysis method to derive a semi-analytic solution. Moreover, the impact of various emerging parameters was elaborately presented. Based on the findings of this investigation, the following conclusions were reached:

1. velocity distribution escalates with a rise in thermal conductivity variation parameter λ, Brinkman number *Br;*
2. velocity distribution reduces with increment in viscosity variation parameter α, thermal radiation parameter *R*, Prandtl number *Pr;*
3. increment is observed in the fluid temperature as a result of increase in thermal conductivity parameter λ, Brinkman number *Br;*

4. viscosity variation parameter α, thermal radiation parameter R, and Prandtl number Pr made temperature profile to decrease.

RECOMMENDATION(S)

Future research could build upon this study by incorporating a moving catalytic plate, examining its influence on the system. This addition offers a new aspect to the investigation, potentially providing valuable information on heat transfer, reaction rates, and its practical implications in areas such as chemical engineering.

REFERENCES

Adegbie, K. S., & Fagbade, A. I. (2016). Analysis of MHD forced convective flow of variable fluid properties over a saturated porous medium with thermal radiation effect. *International Frontier Science Letters, 9*, 47-65.

Adegbie, K. S., Samuel, D. J., & Ajayi, B. O. (2019). Ohmic heating of magnetohydrodynamic viscous flow over a continuous moving plate with viscous dissipation buoyancy and thermal radiation. *Defect and Diffusion Forum, 392,* 73-91.

Ajibade, O. A., & Bichi, Y. A. (2019). Variable fluid properties and thermal radiation effects on natural convective Couette flow through a vertical porous channel. *Journal of Advances in Mathematics and Computer Sciences, 31*(1), 1-17.

Akinbobola, T. E., & Okoya, S. S. (2015). The flow of second-grade fluid over a stretching sheet with variable thermal conductivity and viscosity in the presence of heat source/sink. *Journal of the Nigerian Mathematical Society, 34*(3), 331-342.

Alam, M. S., Sattar, M. A., Rahman, M. M., & Postelnicu, A. (2019). Local similarity solution of an unsteady hydro-magnetic convection flow of micro-polar fluid along continuous moving permeable plate. *International Journal of Heat and Technology, 28*(2), 95-105.

Ali, M. (2017). Similarity solution of unsteady MHD boundary layer flow and heat transfer past a moving wedge in a nanofluid using the Buongiorno Model. *Procedia Engineering, 194*, 407-413.

Babu, R. D. (2020). Similarity solution for unsteady magnetohydrodynamic flow between two parallel porous plates with an angular velocity. *International Journal of Ambient Energy, 20*(12), 330-345.

Bichi, Y. A., & Ajibade, O. A. (2020). Effects of variable viscosity, viscous dissipation, and thermal radiation on unsteady natural convection Couette flow through a vertical porous channel. *FUDMA Journal of Sciences, 4*(2), 135-150.

Cogley, A. C., Vincenti, V. G., & Giles, S. E. (1968). Differential approximation for near-equilibrium flow of a nongray gas. *American Institute of Aeronautics and Astronautics, 6*(1968), 551-553.

Dagan, Y., Greenberg, J. B., & Katoshevski, D. (2017). Similarity solutions for the evolution of polydisperse droplets in vortex flows. *International Journal of Multiphase Flow, 97*, 1-9.

Ebiwareme, L., Kormane, F. P., & Odok, E. O. (2022). Simulation of unsteady MHD flow of incompressible fluid between two parallel plates using Laplace-Adomian decomposition method. *World Journal of Advanced Research and Reviews, 14*(3), 136-145.

Hafees, H. Y., & Ndikilar, C. E. (2014). Flow of viscous fluid between two parallel porous plates with bottom injection and top suction. *Progress in Physics, 10*(1), 49-51.

Hossain, M. T., Mandal, B., & Hoossain, M. A. (2013). Similarity solution of steady combined free and forced convective laminar boundary layer flow about a vertical porous surface with suction and blowing. *Procedia Engineering, 56*, 134-140.

Jenifer, A. S., Saikrishnan, P., & Lewis, R. V. (2021). Unsteady MHD mixed convection flow of water over a sphere with mass transfer. *Journal of Applied and Computational Mechanics, 7*(2), 935-943.

Jha, B. K., Aina, B., & Rilwanu, Z. (2016). Steady fully developed natural convection flow in a vertical annular microchannel having temperature-dependent viscosity: An exact solution. *Alexandria Engineering Journal, 55*(2), 951-958.

Kesavaiah, C. D., & Devika, B. (2020). Free convection and heat transfer of a Couette flow an infinite porous plate in the presence radiation effect. *Journal of Xian University of Architecture and Technology, 10*(5), 525-543.

Koriko, O. K., & Animasaun, I. L. (2017). New similarity solution of micro-polar fluid flow problem over an uhps in the presence of quartic kind of auto-catalytic chemical reaction. *Frontiers in Heat and Mass Transfer, 8*(26), 1-13.

Kudenatti, R. B., Kirsur, S. R., Nargund, A. L., & Bujurke, N. M. (2017). Similarity solutions of the MHD boundary layer flow past a constant wedge within porous media. *Mathematical Problems in Engineering, 2017*, 1-11.

Makinde, O. D., & Animasaun, I. L. (2016). Thermophoresis and Brownian motion effects on MHD bioconvection of nanofluid with nonlinear thermal radiation and quartic chemical reaction past an upper horizontal surface of a paraboloid of revolution. *Journal of Molecular Liquids, 221*, 733-743.

Mohammed, N. U. (2016). Similarity solutions of unsteady mixed convective boundary layer flow of viscous incompressible fluid along isothermal horizontal plate. *Open Journal of Fluid Dynamics, 6*, 279-302.

Opadiran, S., & Okoya, S. S. (2021). Combined effect of fluid's viscous dissipation, variable viscosity, and thermal conductivity on the free convective heat transfer past a circular cylinder. *Journal of the Nigerian Mathematical Society, 40*(3), 321-337.

Philip, K. H., & Hui, V. H. (1990). Similarity solutions of the two-dimensional unsteady boundary-layer equations. *Journal of Fluid Mechanics, 216*, 537-559.

Rani, Y. S. (2019). Jeffrey fluid behavior on oscillatory Couette flow past two horizontal parallel plates in presence of MHD and radiative heat transfer. *International Journal of Innovative Technology and Exploring Engineering, 8*(11), 3252-3257.

Salahuddin, T., Siddique, N., Arshad, M., & Tlili, I. (2020). Internal energy change and activation energy effects on Casson fluid. *Ain Shams Engineering Journal, 10*, 025009.

Salawu, S. O., Oladejo, N. K., & Dada, M. S. (2019). Analysis of unsteady viscous dissipative Poiseuille fluid flow of two-step exothermic chemical reaction through a porous channel with convective cooling. *Ain Shams Engineering Journal, 10*(3), 565-572.

Seth, G. S., Sarkar, S., & Chamkha, A. J. (2016). Unsteady hydromagnetic flow past a moving vertical plate with convective

surface boundary condition. *Journal of Applied Fluid Mechanics, 9*(4), 1877-1886.

Soid, S. K., Ishak, A., & Pop, L. (2017). Unsteady MHD flow and heat transfer over a shrinking sheet with ohmic heating. *Chinese Journal of Physics, 55*(4), 1626-1636.

Umavathi, J. C. (2015). Combined effect of variable viscosity and variable thermal conductivity on double-diffusive convection flow of a permeable fluid in a vertical channel. *Transport in Porous Media, 108*, 659-678.

Zaib, A., Khan, U., Vakif, A., & Zaydan, M. (2020). Numerical entropic analysis of mixed MHD convective flows from a non-isothermal vertical flat plate for radiative tangent hyperbolic blood biofluids conveying magnetite ferroparticles: Dual similarity solutions. *Arabian Journal for Science and Engineering, 45*, 5311-5330.